

See discussions, stats, and author profiles for this publication at: <https://www.researchgate.net/publication/262145400>

pH-Sensitive C-ON Bond Homolysis of Alkoxyamines of Imidazoline Series: A Theoretical Study

ARTICLE in THE JOURNAL OF PHYSICAL CHEMISTRY B · MAY 2014

Impact Factor: 3.3 · DOI: 10.1021/jp5024372 · Source: PubMed

CITATIONS

3

READS

68

4 AUTHORS:



Dmitriy Parkhomenko

Novosibirsk Institute of Organic Chemistry

7 PUBLICATIONS 42 CITATIONS

SEE PROFILE



Mariya Edeleva

International Tomographic Center

8 PUBLICATIONS 73 CITATIONS

SEE PROFILE



Vitaly G Kiselev

Russian Academy of Sciences

27 PUBLICATIONS 216 CITATIONS

SEE PROFILE



E.G. Bagryanskaya

Novosibirsk Institute of Organic Chemistry

136 PUBLICATIONS 1,542 CITATIONS

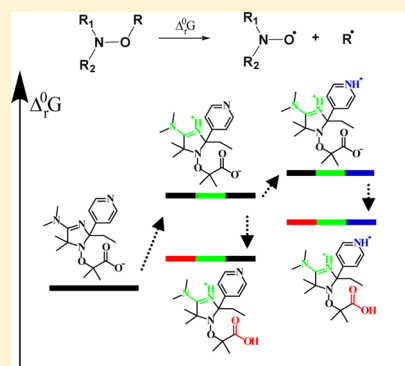
SEE PROFILE

pH-Sensitive C–ON Bond Homolysis of Alkoxyamines of Imidazoline Series: A Theoretical Study

Dmitriy A. Parkhomenko,^{†,‡,§} Mariya V. Edeleva,[§] Vitaly G. Kiselev,^{*,‡,||} and Elena G. Bagryanskaya^{*,†,‡,§}[†]N. N. Vorozhtsov Novosibirsk Institute of Organic Chemistry SB RAS, 9, Lavrentieva Ave., Novosibirsk, 630090 Russia[‡]Novosibirsk State University, 2, Pirogova Str., Novosibirsk, 630090 Russia[§]International Tomography Center SB RAS, 3a, Institutskaya Str., Novosibirsk, 630090 Russia^{||}Institute of Chemical Kinetics and Combustion SB RAS, 3, Institutskaya Str., Novosibirsk, 630090 Russia

S Supporting Information

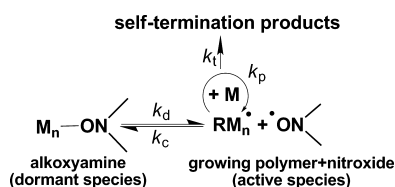
ABSTRACT: The pH-dependent kinetics of C–ON bond homolysis reactions of the four alkoxyamines (viz., the derivatives of 2-(4-(dimethylamino)-2-ethyl-5,5-dimethyl-2-(pyridin-4-yl)-2,5-dihydro-1H-imidazol-1-oxyl and 2-(2-carboxyethyl)-5,5-diethyl-2,4-dimethyl-2,5-dihydro-1H-imidazol-1-oxyl) in water solution have been scrutinized using DFT calculations (M06-2X/6-311++G(2df,p) level of theory with the PCM model). On the basis of computations, the experimental results obtained before (*J. Org. Chem.* **2011**, *76*, 5558) have been rationalized. The concentration dependence of all possible protonated forms of the four alkoxyamines was obtained from pH measurements. The contributions of particular protonated forms into the overall rate constants of thermolysis were estimated using the DFT calculated Gibbs free energies Δ_r^0G of C–ON bond homolysis reactions. The computations revealed that the observed rate constants of thermolysis of the two species at several pH values are dominated by decomposition reactions of two or even three protonated forms. The observed trends in reactivity of the alkoxyamines were mainly attributed to destabilization of the radical products of C–ON bond scission reactions. A linear correlation between the sum of radical stabilization energies (RSEs) of products of thermolysis and the calculated Gibbs free energies of reactions was found for various protonated forms of the species studied. Apart from this, the linear correlation exists between the relative RSE and nitrogen hyperfine constants a_N of various protonated forms of the nitroxide radical products.



■ INTRODUCTION

Controlled radical polymerization (in particular, nitroxide-mediated radical polymerization, NMP) is a promising method yielding polymeric materials with a desired molecular weight, complex structure, and reactive end groups.^{1,2} The simplified kinetic model of NMP polymerization is shown in Scheme 1.

Scheme 1. Simplified Kinetic Scheme of Nitroxide Mediated Polymerization



The key process in the kinetic scheme of NMP is the reversible recombination of growing chain alkyl radicals M_n with persistent nitroxide radical species to dormant polymer chains (Scheme 1). Note that the efficiency of NMP strongly depends on the rate constants of homolysis of dormant species (alkoxyamines) k_d and recombination of the nitroxyl and alkyl radicals k_c (Scheme 1).³ Therefore, the particular

controlling agent determines the equilibrium constant $K = k_d/k_c$ of alkoxyamine homolysis (Scheme 1) and, ultimately, whether the polymerization occurs in the “living” regime. Consequently, during the last decades significant effort has been spent toward development of initiator/controlling agents of NMP.^{4–10}

The rate constants k_d and k_c are naturally dependent on the structure of a particular monomer. Therefore, the polymerization of particular monomers in the controlled mode usually requires the use of different nitroxide agents. However, Rizzardo et al.^{11–13} have recently introduced a new concept of pH-switchable agents for reversible addition–fragmentation chain transfer (RAFT) polymerization. In the framework of this concept, the same mediator is employed for various monomers. The desired ratios of the rate constants are adjusted by varying the protonation state of the RAFT agents, which, in turn, is controlled by the pH of the solvent. For instance, it has been shown¹³ that the kinetic parameters of the RAFT polymerization process can vary (some rate constants - up to seven

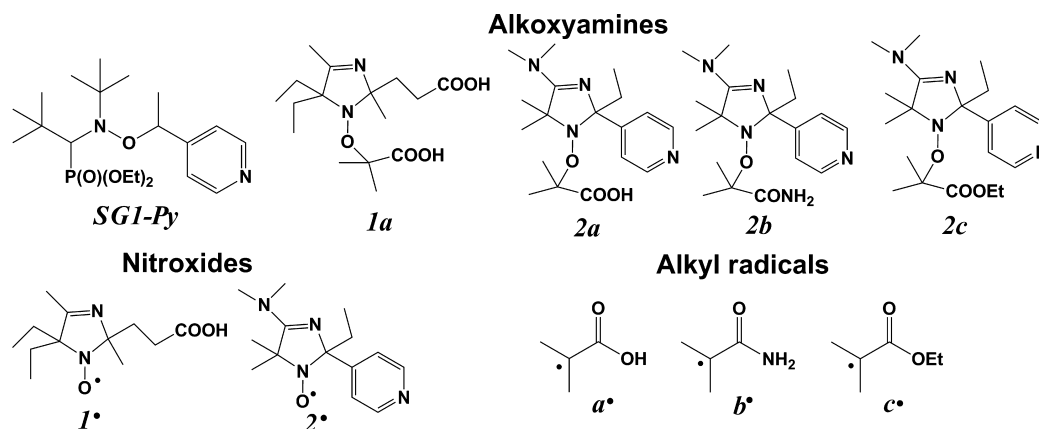
Received: March 11, 2014

Revised: April 25, 2014

Published: April 29, 2014



Chart 1



times) upon protonation of the monomeric species. Moreover, the authors^{11–13} were able to perform polymerization of the so-called “more activated” (e.g., styrene, methyl acrylate) and “less activated” (e.g., vinyl acetate, *N*-vinylpyrrolidone) monomers using the same universal controlling agent, viz., dithiocarbamate in protonated and deprotonated forms, at various pH values.

Recently, the idea of pH-switchable controlling agent has been implemented in the NMP process. Marque et al.^{14–16} studied the influence of protonation of the nitrogen atom in the pyridine moiety of an alkoxyamine SG1-Py (Chart 1) on the homolysis rate constant k_d (Scheme 1). The k_d value of the protonated alkoxyamine turned out to be 64 times higher than its counterpart of the deprotonated form at 75 °C.¹⁵ The authors suggested^{15,16} that the protonation of SG1-Py leads to destabilization of the reactant due to polar effects along with stabilization of the alkyl radical. These two factors result in decrease in the C–ON bond energy and, consequently, lead to increase in the observed k_d value upon protonation.

Furthermore, Edeleva et al. have recently shown¹⁷ that the k_d values of alkoxyamines 1a–2c with a pH-sensitive imidazoline nitroxide moiety containing several protonation/deprotonation centers (Chart 1) differ by more than one order of magnitude at various pH. It was also found that the protonation of nitroxyl moiety of alkoxyamine decreases the homolysis rate constant k_d and has virtually no effect on the recombination rate constant k_c . However, even though the authors¹⁷ measured the overall rate constant k_d , they were not able to separate the contributions of particular protonated forms of 1a–2c to the observed rate constant k_d . Apart from this, pH-sensitive nitroxides of imidazoline and imidazolidine series^{18,19} were successfully employed in the NMP of water-soluble monomers (viz., sodium 4-styrenesulfonate and acrylates)¹⁷ and their copolymers.

It should be emphasized that thermodynamics and rate constants of elementary reactions (in particular, C–ON bond homolysis) are crucial for modeling the complex process of NMP and design of new promising agents. However, the available experimental data¹⁷ on the primary thermal decomposition reactions of the alkoxyamines 1a–2c are incomplete. For example, it is hard to separate clearly the contributions of all protonated/deprotonated forms into the apparent rate constant of homolysis. In this case, quantum chemical calculations are the most appropriate alternative for study of the elementary reactions. For instance, the C–ON bond dissociation energies for a series of alkoxyamines have recently been calculated using a variety of DFT methods and

G3(MP2)-RAD multilevel procedure.²⁰ Moreover, the stability of various distonic nitroxide radical anions has recently been carefully scrutinized.^{21,22} However, to the best of our knowledge, the C–ON bond scission in various protonated forms of alkoxyamines with ionizable group in the nitroxide moiety has never been considered.

The main goals of the present contribution are to study experimentally and theoretically the pH concentration dependence of different possible protonated forms of alkoxyamines 1a–2c to identify clearly the elementary rate constants of C–ON bond scission reactions of these forms and ultimately to give deeper mechanistic insight into the kinetics of thermolysis of the species studied. To this end, the pH measurements and quantum chemical (DFT) computations were employed. First, we carefully measured the concentrations of various protonated forms of 1a–2c. Afterward, we calculated the Gibbs free energies of the primary homolysis reactions of all protonated forms in solution. The obtained results were correlated with radical stabilization energies of products and hyperfine constants. In contrast with all previous publications, we considered in detail the reactions of various protonated forms of alkoxyamines and demonstrated their importance at particular pH values.

■ EXPERIMENTAL AND COMPUTATIONAL DETAILS

Quantum Chemical Calculations. The geometry optimizations and frequency calculations of the alkoxyamines and radical products made use of the Truhlar’s group M06-2X density functional²³ and the 6-31G(d) basis set. All equilibrium and transition-state structures were ascertained to be the minima or saddle points, accordingly, on the potential energy surfaces (PESs). The corresponding thermal corrections calculated using the harmonic oscillator-rigid rotor (RRHO) assumption were included to obtain the enthalpy and Gibbs free energy values at 298 K. The values of energy were then refined at the M06-2X/6-311++G(2df,p) level of theory. Note that the M06-2X functional was found to perform quite well on a test set of reactions of various TEMPO-alkylalkoxyamines.²⁰ Moreover, it has been recently demonstrated that the latter functional correctly reproduces the trends in the bond dissociation energies of a series of protonated/deprotonated alkoxyamines.²¹

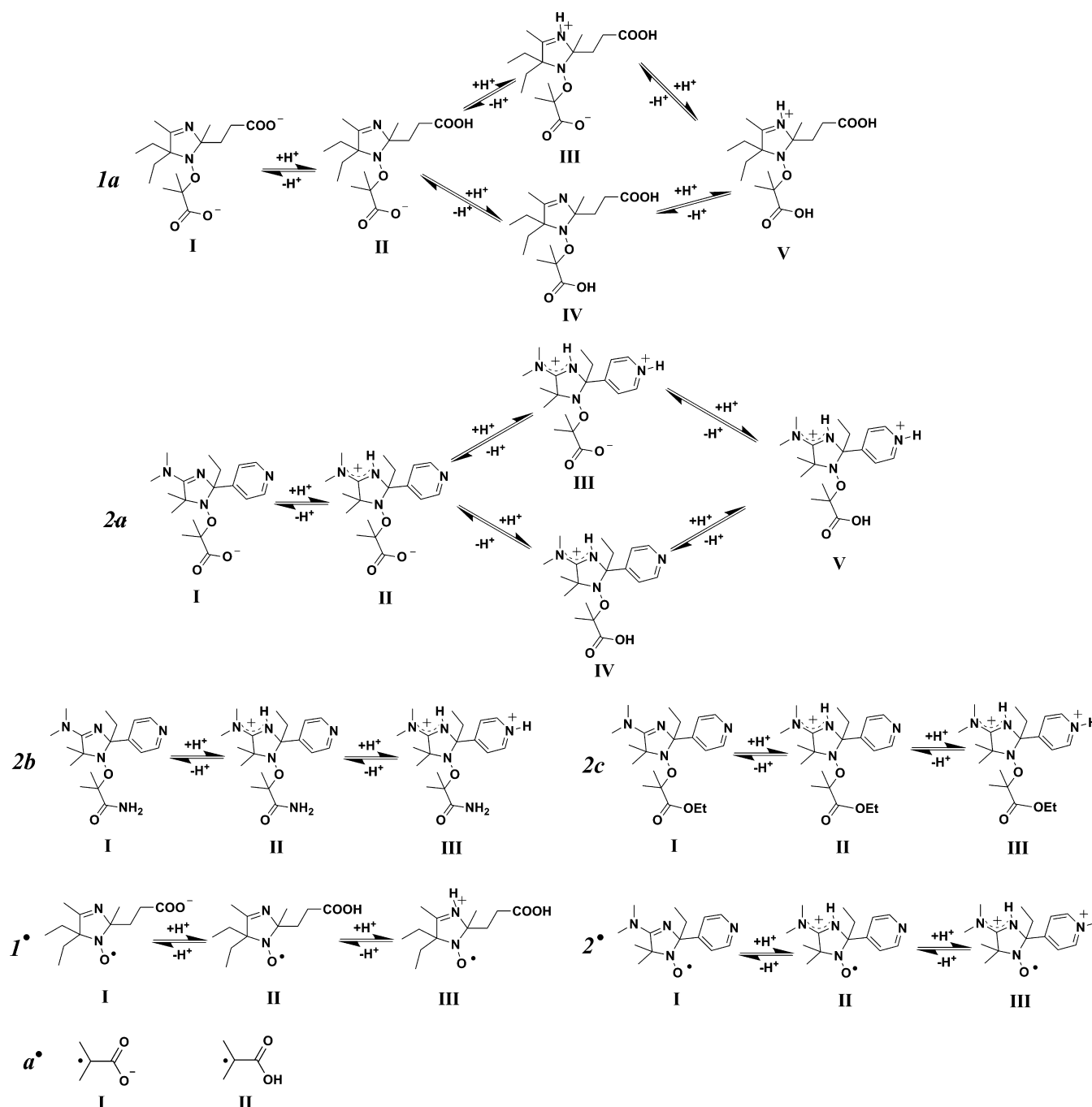
The influence of the solvent on thermochemistry and rate constants was taken into account by the calculation of the free energies of solvation. These values were computed at the M06-2X/6-311++G(2df,p) level of theory using the PCM model²⁴

Table 1. pK_a Values of the Functional Groups of Alkoxyamines 1a–2c^a

compound	pK_{a1}	pK_{a2}	pK_{a3}	solvent	method
1a	3.7 ^b	5.7 ^b	4.0 ^b	D ₂ O	¹ H NMR
2a	9.8 ^b	5.25 ^b	4.0 ^c	D ₂ O	¹ H NMR
2b	8.0 ^b	5.0 ^b	0.0 ^c	D ₂ O	¹ H NMR
2c	7.8 ^d	3.3 ^d		D ₂ O/MeOD (1:1 v/v)	¹ H NMR
	7.5 ^d	3.3 ^d		H ₂ O/EtOH (1:1 v/v)	UV–vis

^a pK_{a1} refers to protonation of the nitroxide ring (see Chart 1 for the details of structure), pK_{a2} refers to protonation in the nitroxyl moiety, and pK_{a3} refers to deprotonation in the alkyl moiety (no groups to be deprotonated in 2c). ^bRef 17. Note that the pK_a values for 1a are misprinted in ref 17.

^cThese values were proposed using the literature data for the similar species, cf. the Discussion in the text. ^dThis work; see the Supporting Information for details (Figures S1 and S2).

Scheme 2. Protonated/Deprotonated Forms of the Alkoxyamines 1a–2c, nitroxide radicals 1[•], 2[•], and alkyl radical a[•] existing in the pH range 2.0–11.0

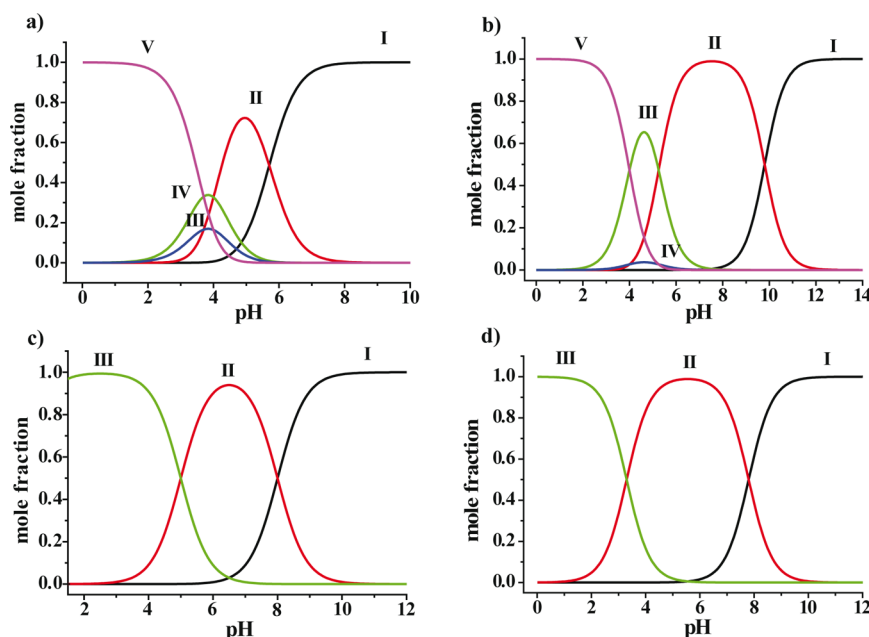


Figure 1. Concentrations (mole fractions) of various protonated/deprotonated forms of **1a** (a), **2a** (b), **2b** (c), and **2c** (d) in the D_2O solution ($D_2O/MeOD$ in the case of **2c**) at different pH values.

and water as a solvent. The solution-phase free energies were calculated as the sum of the corresponding gas-phase free energy, the free energy of solvation, and a correction term $RT \ln(RT/P^0)$, where R is the ideal gas constant, T is the reaction temperature, and P^0 is the standard pressure of 1 atm (101.325 kPa). The correction term accounts of the standard-state concentration difference between the gas and solution (1 atm and 1 M, correspondingly).²⁵ It has also been noted that the explicit consideration of water molecules improves the accuracy of computations in the case of several nitroxide species.²⁶ Therefore, we considered the complexes of the compounds studied with three water molecules. All other solvation shells were accounted by the PCM model. All calculations have been performed using Gaussian 09 suite of programs.²⁷

The radical stabilization energy (RSE)^{28,29} was calculated as the Gibbs free energy $\Delta_r G$ (including the free energy of solvation) of the isodesmic reaction 1. The reference radical $\bullet X = \bullet CH_3$ was employed.



pK_a Measurements. The pK_a values of the alkoxyamines studied were determined by either 1H NMR or UV-vis spectroscopy. The solution of 20 mM of an alkoxyamine **2c** (Chart 1) in $D_2O/MeOD$ (1/1 v/v) mixture was used in 1H NMR experiments, and the 10^{-4} M solution of **2c** in water/ethanol mixture was used in the UV-vis measurements, correspondingly. In both cases, HCl and NaOH were used to adjust the pH value. The conventional glass electrode calibrated using commercial buffer solutions was used for pH measurements. The pH values for deuterated solvents were reported without corrections. All NMR spectra were recorded with the Bruker Avance 200 MHz NMR spectrometer. The UV measurements were performed using the Agilent 8453E spectrophotometer.

RESULTS AND DISCUSSION

1. Experimental Study of pK_a and Concentrations of Various Protonated/Deprotonated Forms of **1a–2c.** At first, we obtained the pK_a values of alkoxyamines **1a–2c** (Chart 1) using the UV-vis and 1H NMR spectroscopies. (The details are presented in the Supporting Information, Figures S1–S2.) The results along with the data from our previous work¹⁷ are given in Table 1. Note that the presence of several NMR lines in the vicinity of typical region of 1 to 2 ppm (CH_3 protons) resulted in quite complicated NMR spectra (figure 2 in ref 17). Therefore, we were not able to determine the pK_{a3} of a carboxylic group in the alkyl part of **2a** (Table 1). However, it is reasonable to expect this value to be close to the corresponding pK_{a3} of that group in **1a** (Table 1). pK_{a3} of an acetamide group of **2b** was proposed to be close to zero.³⁰ Therefore, we hypothesized this group to be deprotonated under NMP conditions. It is also worth mentioning that the NMP experiments are typically performed in an H_2O solution. Therefore, in the case of **2c**, we compared the 1H NMR (D_2O solution) and UV-vis (H_2O solution) titration curves. It is seen from Table 1 that the pK_a values obtained using both techniques are close to each other. Therefore, we used the 1H NMR values for all further calculations.

In general case, there are four and eight possible protonated forms of the alkoxyamines containing two and three ionizable groups, respectively. Using the measured pK_a values of these groups (Table 1), we calculated the concentrations of all possible forms in the range of pH values from 2.0 to 11.0 employed in our experiments. (The details of calculations are given in Section 2 of the Supporting Information.) Five protonated/deprotonated forms of **1a** and **2a** turned out to exist in noticeable concentrations under experimental conditions and three forms existed in the case of **2b** and **2c**, respectively (Scheme 2). The concentrations of other forms were profoundly lower than those of the former species. Therefore, we studied in detail the species depicted in Scheme 2.

Table 2. Percentage of Different Protonated/Deprotonated Forms of the Alkoxyamines 1a–2c, Rate Constants of C–ON Bond Homolysis k_d , and Activation Energies E_a

species	form ^a	solvent and pH	T, K	$k_d \times 10^4, s^{-1b}$	$E_a, kcal/mol^c$
1a	V, IV, III (75.6%, 15.1%, 7.6%)	D ₂ O, pH 3.0	368	1.2 ± 0.1	
	II, I, IV, III (69.3%, 21.9%, 4.4%, 2.2%)	D ₂ O, pH 5.2		4.2 ± 0.2	
	I	D ₂ O, pH 9.5		14.0 ± 0.5	29.0
2a	V, III (90.4%, 9%)	D ₂ O, pH 3.0	368	2.6 ± 0.1	30.2
	II, III (96.3%, 3.4%)	D ₂ O, pH 6.7		12.0 ± 0.5	29.1
	II, I (92.6%, 7.4%)	D ₂ O, pH 8.7		35 ± 2	
	I, II (94%, 6%)	D ₂ O, pH 11.0		45 ± 2	28.2
2b	III	D ₂ O, pH 1.5, pH 3.0	363	0.20 ± 0.02	31.7
	II	D ₂ O, pH 7.0		0.55 ± 0.01	31.0
	I	D ₂ O, pH 10.0		1.3 ± 0.1	30.1
2c	III	D ₂ O:CD ₃ OD = 1:1, pH 3.0	368	0.5 ± 0.05	30.8
	II	D ₂ O:CD ₃ OD = 1:1, pH 6.7		3.0 ± 0.5	29.6
	I	D ₂ O:CD ₃ OD = 1:1, pH 8.7		5.0 ± 0.5	29.4

^aAll forms are named in accordance with Scheme 2. The contributions higher than 2% are listed. ^bThe experimentally measured rate constants are from ref 17. ^cThe activation energies were calculated assuming the Arrhenius temperature dependence of the rate constants $k = A \exp(-E_a/RT)$ with an average preexponential factor $A = 2.4 \times 10^{14} s^{-1}$ (ref 31).

Figure 1 represents pH concentration dependences for all protonated/deprotonated forms from Scheme 2. (Recall that the details of calculations are given in the Supporting Information, Section 2.) Because the pK_a values of 1a are close to each other ($pK_{a1} = 3.7$ and $pK_{a3} = 4.0$, Table 1), the four protonated forms of 1a coexist in the pH range of 3.0–5.0 (Figure 1a, Scheme 2). In the case of 2a, the three forms have noticeable concentrations in the same pH range, and two forms have notice concentrations in the pH values from 5.0 to 11.0 (Figure 1b, Scheme 2). On the other hand, 2b and 2c exist almost entirely in a single form at typical pH values of 3.0, 6.0, and 10.0 (Figure 1c,d).

2. Kinetics of Homolysis of 1a–2c at Various pH Values and Contributions of Individual Protonated Forms: Comparison of Experimental and Calculated Data. Having calculated the pH concentration dependences, we scrutinized the kinetics of thermolysis of 1a–2c. The C–ON bond homolysis yielding nitroxide (1• and 2•) and alkyl radicals (a•–c•, Chart 1) is known to be the dominating primary decomposition reaction of the latter alkoxyamines.⁵ The experimentally measured¹⁷ first-order rate constants of homolysis k_d along with a percentage of protonated forms at various pH values are given in Table 2.

Note that in the present work we clearly separated the contribution of various protonated forms of 1a–2c at different pH values. Taking into account the presence of several protonated forms of alkoxyamines at a given pH, the experimentally measured rate constant of homolysis k_d reads as

$$k_d = \sum_i A_i k_d^i \quad (2)$$

where A_i is a mole fraction (cf. Figure 1) and k_d^i is the rate constant of elementary decomposition reaction of the protonated form i .

It is seen from Table 2 that in the case of 2b and 2c the experimental k_d values at different pH (Table 2) values correspond to a single protonated form of these species (cf. Figure 1). Therefore, the values given in Table 2 are true elementary rate constants of homolysis k_d^i of different protonated states of 2b and 2c. Using formula 2 and the pH concentration dependence of I–III species (Figure 1c,d), we calculated the effective k_d values of 2b and 2c in the whole

range of pH (Figure S3 in the Supporting Information). The details of calculations are also given in the Supporting Information, section 3.

It is worth mentioning that the activation energies obtained before¹⁷ for 1a do not correspond to a particular protonated form and are effective values in accordance with equation 2. For example, in contrast with the previous assumptions,¹⁷ the three forms of 1a turned out to coexist at the pH values of 3.0 and 5.2 (Figure 1a, Table 2). In the case of 2a, the percentage of a particular single form is more than 90% in each case (Table 2). However, the concentrations of other forms are non-negligible (Table 2). It is therefore hard to extract the reliable k_d^i values for each protonated form of 1a and 2a from the experimental data.¹⁷ Therefore, in the last column of Table 2, we present only the activation energies that correspond to the reactions of a single dominating protonated/deprotonated form of the species 1a–2c (cf. the Discussion later).

To get deeper insight into the decomposition kinetics of each particular protonated form of the alkoxyamines studied, we performed quantum chemical calculations of some relevant points on the PES of the latter species. Note that the recombination reactions of alkyl and nitroxyl radicals are typically barrierless.^{32–36} It is therefore reasonable to expect the radical decomposition reactions of 1a–2c to be barrierless as well. In this case, the accurate computation of the rate constant (e.g., using variational transition state theory, VTST)³⁷ is a rather demanding procedure. Therefore, a simplified approach was applied: namely, we calculated the Gibbs free energies $\Delta_r^0 G$ of homolysis reactions in the water solution using the M06-2X functional and PCM model and assumed a correlation between $\Delta_r^0 G$ and the activation barriers of these reactions. It should be emphasized that the computed $\Delta_r^0 G$ values cannot be directly compared with the activation energies for two principal reasons. First, in accordance with the VTST,³⁷ the Gibbs free energy of reaction $\Delta_r^0 G$ is the *lower estimate* of the Gibbs free energy of activation $\Delta^\ddagger G_0$. Moreover, the $\Delta_r^0 G$ values of monomolecular decomposition reactions are typically profoundly lower^{38,39} than the corresponding reaction enthalpies $\Delta_r^0 H$ due to higher contributions of translational degrees of freedom into the entropy of products. Apart from this, the activation energies from Table 2 were estimated using the only value of the rate

constant at a fixed temperature. The uncertainties of such estimates of activation energies might therefore be significant.

It is also worth mentioning that most of the species under study have two or more conformers. Only properties of the lowest energy conformers will be discussed henceforth. The geometries of all compounds under study optimized at the M06-2X/6-31G(d) level of theory are given in the Supporting Information (Section S).

Table 3 represents the DFT calculated $\Delta_r G$ values of the homolysis reactions of all possible protonated states of

Table 3. Gibbs Free Energies $\Delta_r G$ of C–ON Bond Homolysis Reactions in Water Solution of Various Protonated Forms of 1a–2c Calculated at the M06-2X/6-311++G(2df,p) Level of Theory^a

alkoxyamine	protonated/deprotonated form ^b	$\Delta_r G$, kcal/mol
1a	I	20.9
	II	19.1
	III	21.6
	IV	18.0
	V	21.0
2a	I	21.4
	II	24.7
	III	25.0
	IV	22.6
	V	24.3
2b	I	22.4
	II	24.3
	III	25.2
2c	I	17.5
	II	19.9
	III	20.7

^aSolvation energies were computed using the PCM model at the same level of theory. All Values are in kilocalories per mole. ^bAll forms are named in accordance with Scheme 2.

alkoxyamines 1a–2c (Scheme 2). It is seen from Table 3 that $\Delta_r G$ increases upon sequential protonation of nitroxyl moiety of all compounds studied (cf. Scheme 2). Note that in the case of 2b and 2c, the increase in $\Delta_r G$ upon protonation (Table 3) agrees well with the decrease in the rate constants observed experimentally (Table 2, Figure S3 in the Supporting Information). In the case of alkoxyamines 1a and 2a, the deprotonation of carboxylic group in the alkyl moiety (species IV and II or V and III, Scheme 2) slightly increases $\Delta_r G$ as well (Table 3). The typical case of 2a is shown in Figure 2. These trends are entirely consistent with the previous findings for studied compounds.^{15,17}

The data from Tables 2 and 3 allow for detailed understanding of the experimental kinetics observed at various pH for 1a and 2a. Namely, in the case of 1a, at pH 3.0 the protonated form V is the most abundant (~76%) and the neutral form IV comprises ~15%. At the same time, the calculated Gibbs free energy of thermolysis of IV is 3 kcal/mol lower than that of V (Table 3). It is therefore seen that the thermal decomposition of 1a at low pH values is dominated by the two forms IV and V. Both of them contribute to the observed rate constant (Table 2) as a result of a tiny interplay between pH-dependent concentrations and elementary rate constants of decomposition of particular forms.

At pH 5.2, the most abundant form of 1a is II (~70%, Table 2). The next in concentration (~22%, Table 2) is the

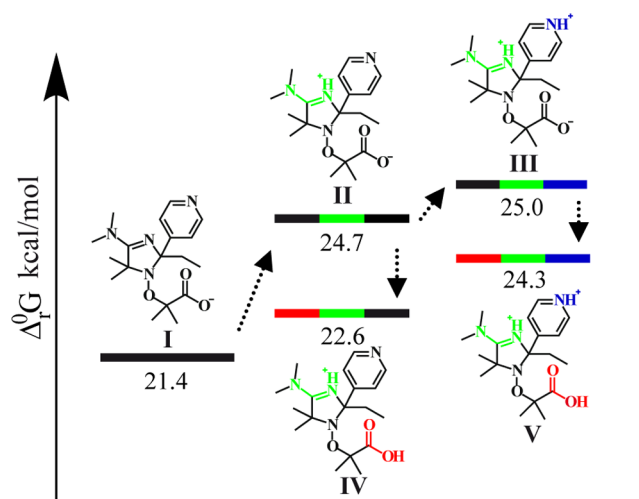


Figure 2. Schematic of the Gibbs free energies $\Delta_r G$ of C–ON bond homolysis reactions in water solution of various protonated forms of 2a calculated at the M06-2X/6-311++G(2df,p) level of theory. The solvation energies were computed using the PCM model at the same level of theory (black, a deprotonated group; green, a protonated amidine group; blue, a protonated pyridine group; red, a protonated carboxylic group).

deprotonated form I. Given the fact that $\Delta_r G$ value of I is ~2 kcal/mol higher than that of II (Table 3), we suggest the form I to be kinetically unimportant. However, the calculated Gibbs free energy of thermolysis of IV (~4%, Table 2) is ~1 kcal/mol lower than that of II. Therefore, the species IV, although existing in low concentrations at pH 5.2, might contribute noticeably to the effective rate constant of C–ON bond homolysis (eq 2).

The experimental data at pH 9.5 (Table 2) give additional evidence to this assumption. It is seen from Table 2 that thermolysis of 1a at pH 5.2 (the concentration of the form II is ~70%, of the form I ~22%) occurs *slower* than that at pH 9.5 (the form I comprises ~100%). At the same time, as was previously mentioned, the calculated $\Delta_r G$ value for I of 1a is *higher* than that for form II (Table 3). Therefore, the presence of another form at pH 9.5, even in a tiny concentration, is crucial for understanding the kinetics of thermolysis of 1a. On the other hand, the computed value for the form I might not obey the general trends (see a discussion below).

In contrast with the case of 1a, the observed rate constants of thermolysis of 2a at various pH values (Table 2) correspond mainly to a single protonated form. At pH 3.0, the doubly deprotonated form V comprises 90%, and the calculated $\Delta_r G$ value for this species is slightly lower than that for the form III, which comprises 9% (Tables 2 and 3). Therefore, only the species V is important for the kinetics of thermolysis. Similarly to this case, the zwitterionic form II dominates the kinetics at pH 6.7, and the form I dominates the kinetics at pH 11.0 (Tables 2 and 3). However, at pH 8.7 the forms II and I exist in the mole fractions ~93 and ~7%, respectively, while the calculated $\Delta_r G$ value of I is 3.3 kcal/mol lower than that of II. Thus, it is reasonable to expect that both forms contribute noticeably into the observed rate constant (eq 2).

3. Stability of Radical Products: Correlation between Radical Stabilization Energies, Hyperfine Constants, and Gibbs Free Energies of C–ON Homolysis Reactions. Having obtained the kinetics of thermolysis of various protonated forms of 1a–2c, we tried to rationalize our findings.

Table 4. Radical Stabilization Energies (RSE) and Nitrogen Hyperfine Coupling Constants (a_N) for Nitroxide Radicals 1^\bullet , 2^\bullet in Different Protonated Forms and Alkyl Radicals a^\bullet , b^\bullet , and c^\bullet ^a

radical	CH_3^b	1^\bullet			2^\bullet			a^\bullet		b^\bullet	c^\bullet
		I	II	III	I	II	III	I	II		
RSE, kcal/mol	0	32.2	31.6	27.3	37.4	33.9	31.8	15.1	16.2	15.2	16.4
a_N , G		15.10 ^c	15.00 ^c	13.96 ^c	15.31 ^d	14.50 ^d	13.97 ^d				

^aNotations are in accordance with Chart 1 and Scheme 2. ^bMethyl radical was chosen as a reference species for computations of the relative thermodynamic properties. ^cRef 43. ^dRef 17.

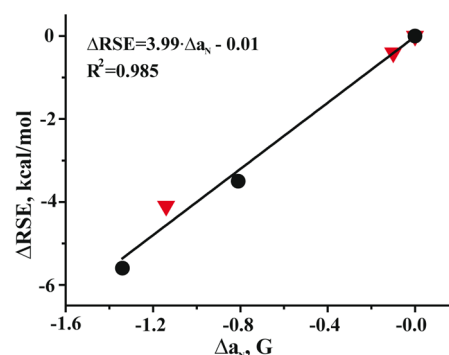
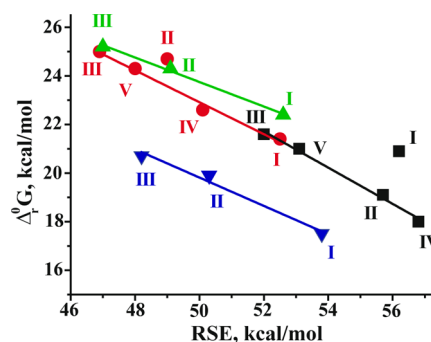
Ultimately, we aimed at understanding whether the observed trends in the kinetics of thermolysis of various protonated/deprotonated species were caused by an intrinsic stability of reagents (alkoxyamines **1a–2c**) or by a (de)stabilization of radical products (nitroxide and alkyl radicals). To this end, the concept of the radical stabilization energy (RSE) has been applied. The RSE is commonly used to estimate relative stability of radicals.^{40–42} Note that the RSE is usually defined as the enthalpy change in the isodesmic reaction 1. To take the influence of solvent into account, we use hereafter the modified definition of RSE as the Gibbs free energy Δ_r^0G (including the free energy of solvation) of reaction 1.

It is seen from Table 4 that protonation of alkoxyamines **1a–2c** noticeably changes the RSE values of radical products (1^\bullet – 2^\bullet , a^\bullet – c^\bullet) of their thermolysis. Protonation of nitroxide radicals decreases the RSE (Table 4). This fact infers destabilization of these species upon protonation. In contrast, protonation of the alkyl radical a^\bullet (Table 4) slightly increases the RSE value and therefore stabilizes a^\bullet . It should be emphasized that the geometry (viz., bond lengths, angles, etc.) and NBO charges on the corresponding atoms do not change noticeably upon protonation/deprotonation (Supporting Information, Section 4). Therefore, we infer that the (de)stabilization of the radical products determines the observed trends (cf. Tables 2 and 3 and the previous Discussion) in the kinetics of C–ON homolysis of **1a–2c**.

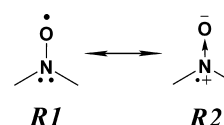
It is worth mentioning that the RSE of various protonated forms of **1** and **2** correlates with the hyperfine constant (HFC) on the nitrogen atom a_N (Table 4). Note that similar decrease of HFC upon protonation has been observed for related nitroxide radicals (viz. derivatives of imidazole⁴³ and imidazolidine⁴⁴ nitroxides). The hyperfine constant is, in turn, proportional to the spin density localized on the nitrogen atom. Therefore, this fact indicates a shift of spin density to the oxygen atom. Consequently, the higher extent of localization of an unpaired electron on the oxygen atom increases the reactivity of nitroxide radical. This fact is also in a good agreement with an observed increase in nitroxide and alkyl radical cross-recombination rate constant k_c upon protonation of the nitroxide radical. (The k_c was much lower than the diffusion rate constant).¹⁷ At the same time, in the case of k_c close to the diffusion limit, no noticeable changes were observed upon protonation.¹⁷ It is also noteworthy that the linear correlation exists between the relative values of RSE and HFC of nitroxides 1^\bullet and 2^\bullet (Figure 3).

Furthermore, Figure 4 represents the correlation between the RSE of the radical products of thermolysis reactions of **1a–2c** (Table 4) and the calculated Gibbs free energies of these reactions (Table 3). It is seen from Figure 4 that the linear correlations were observed for almost all compounds studied. The only two outliers are the forms I of **1a** and II of **2a**.

It is therefore reasonable to infer that the observed reactivity trends of **1a–2c** (Table 3) are mainly due to destabilization of

**Figure 3.** Linear correlation between relative RSE and nitrogen hyperfine coupling constants a_N upon protonation of the nitroxide radicals 1^\bullet (red triangles) and 2^\bullet (filled circles).**Figure 4.** Dependence of the calculated Δ_r^0G of thermolysis reactions of protonated alkoxyamines on the RSE of the nitroxide and alkyl radicals: \blacksquare , **1a** (black); \bullet , **2a** (red); \blacktriangle , **2b** (green); \blacktriangledown , **2c** (blue). The notations are in accordance with Scheme 2.

radical products 1^\bullet and 2^\bullet upon protonation. This destabilization, in turn, correlates with a value of spin density on the oxygen moieties of the nitroxide radicals 1^\bullet and 2^\bullet (Figure 3). Note that the protonation might contribute to radical stability in the two opposite ways. Namely, there are two possible resonance forms for nitroxide radicals (Chart 2). The presence of remote positive charges disfavors the charged form **R2** and therefore reduces the extent of resonance stabilization of 1^\bullet and 2^\bullet . The remote charges render the charge redistribution in radicals, which contributes to a higher stabilization of 1^\bullet and 2^\bullet . The correlation between the HFC a_N (ultimately, the spin density on a nitrogen atom) and RSE (Figure 3) gives

Chart 2

additional evidence to this fact. Therefore, the observed trends (Figures 3 and 4) are a result of a tiny interplay of these two factors. Nevertheless, more detailed studies employing a larger set of nitroxides are indeed necessary to clarify this issue.

CONCLUSIONS

In the present contribution, we studied the kinetics of thermolysis of a series of various protonated forms of alkoxyamines **1a–2c**. To rationalize the observed experimental data, we used the DFT calculated Gibbs free energies Δ_r^0G of C–ON bond homolysis reactions. The computations revealed that the observed rate constants of thermolysis of **1a** and **2a** at several pH values are dominated by decomposition reactions of two or even three protonated forms of these species. Therefore, the activation energies reported before¹⁷ are effective values and do not correspond to a particular elementary reaction. On the contrary, in the case of **2b** and **2c** the experimental k_d values correspond to a single protonated form of these species. Nevertheless, the changes in the calculated Gibbs free energies of thermolysis upon protonation of reagents are in line with experimental trends, viz., decrease in k_d value upon protonation of the nitroxyl moiety.

Furthermore, the observed trends in reactivity of **1a–2c** were mainly attributed to changes in radical stabilization energies (RSEs). We found a linear correlation between the total RSE value of radical products of thermolysis and the calculated Δ_r^0G values for various protonated forms of the compounds studied.

Moreover, linear correlations exist between the relative RSE and nitrogen HFI constants a_N of various protonated forms of the nitroxide radicals **1•** and **2•**. Note that the HFI constants a_N of stable nitroxide radicals can be obtained experimentally in a relatively straightforward way. Thus, on the basis of these facts we propose the variation of a_N upon protonation of the nitroxide radicals to be a useful descriptor for a screening among promising pH-switchable nitroxides (i.e., with the most pronounced changes of k_d upon protonation) for NMP.

ASSOCIATED CONTENT

Supporting Information

Details of pK_a measurements, calculations of pH concentration dependence of protonation forms of **1a–2c**, pH dependence of k_d rate constant of **2b** and **2c**, and optimized geometries of the compounds studied. This material is available free of charge via the Internet at <http://pubs.acs.org>.

AUTHOR INFORMATION

Corresponding Authors

*E-mail: vitaly.kiselev@kinetics.nsc.ru (V.G.K.).

*E-mail: egbagryanskaya@nioch.nsc.ru (E.G.B.).

Notes

The authors declare no competing financial interest.

ACKNOWLEDGMENTS

The funding by RFBR (projects 12-03-01042a and 12-03-31363), RF President's grant MK-1654.2013.3, and the Ministry of Education and Science of the Russian Federation is gratefully acknowledged. This work was also supported by the Siberian Supercomputer Center.

REFERENCES

(1) Solomon, D. H.; Rizzardo, E.; Cacioli, P. Polymerization Process and Polymers Produced Thereby. U.S. Patent 4,581,429, 1986.

(2) Chenal, M.; Boursier, C.; Guillauneuf, Y.; Taverna, M.; Couvreur, P.; Nicolas, J. First Peptide/Protein PEGylation with Functional Polymers Designed By Nitroxide-Mediated Polymerization. *Polym. Chem.* **2011**, *2*, 1523–1530 and references therein..

(3) Souaille, M.; Fischer, H. Kinetic Conditions for Living and Controlled Free Radical Polymerizations Mediated by Reversible Combination of Transient Propagating and Persistent Radicals: The Ideal Mechanism. *Macromolecules* **2000**, *33*, 7378–7394.

(4) Hawker, C. J.; Bosman, A. W.; Harth, E. New Polymer Synthesis by Nitroxide Mediated Living Radical Polymerizations. *Chem. Rev.* **2001**, *101*, 3661–3688.

(5) Nicolas, J.; Guillauneuf, Y.; Lefay, C.; Bertin, D.; Gimes, D.; Charleux, B. Nitroxide-Mediated Polymerization. *Prog. Polym. Sci.* **2013**, *38*, 63–263.

(6) Rizzardo, E.; Solomon, D. H. On the Origins of Nitroxide Mediated Polymerization (NMP) and Reversible Addition–Fragmentation Chain Transfer (RAFT). *Aust. J. Chem.* **2012**, *65*, 945–969.

(7) Sciannamea, V.; Jerome, R.; Detrembleur, C. In-Situ Nitroxide-Mediated Radical Polymerization (NMP) Processes: Their Understanding and Optimization. *Chem. Rev.* **2008**, *108*, 1104–1126.

(8) Bertin, D.; Gimes, D.; Marque, S. R. A.; Tordo, P. Kinetic Subtleties of Nitroxide Mediated Polymerization. *Chem. Soc. Rev.* **2011**, *40*, 2189–2198.

(9) Harrisson, S.; Couvreur, P.; Nicolas, J. Use of Solvent Effects to Improve Control Over Nitroxide-Mediated Polymerization of Isoprene. *Macromol. Rapid Commun.* **2012**, *33*, 805–810.

(10) Bentein, L.; D'hooge, D. R.; Reyniers, M.; Marin, G. B. Kinetic Modeling as a Tool to Understand and Improve the Nitroxide Mediated Polymerization of Styrene. *Macromol. Theory Simul.* **2011**, *20*, 238–265.

(11) Benaglia, M.; Chiefari, J.; Chong, Y.; Moad, G.; Rizzardo, E.; Thang, S. Universal (Switchable) RAFT Agents. *J. Am. Chem. Soc.* **2009**, *131*, 6914–6915.

(12) Benaglia, M.; Chen, M.; Chong, Y.; Moad, G.; Rizzardo, E.; Thang, S. Polystyrene-block-poly(vinyl acetate) through the Use of a Switchable RAFT Agent. *Macromolecules* **2009**, *42*, 9384–9386.

(13) Keddie, D. J.; Guerrero-Sanchez, C.; Moad, G.; Mulder, R. J.; Rizzardo, E.; Thang, S. H. Chain Transfer Kinetics of Acid/Base Switchable N-Aryl-N-Pyridyl Dithiocarbamate RAFT Agents in Methyl Acrylate, N-Vinylcarbazole and Vinyl Acetate Polymerization. *Macromolecules* **2012**, *45*, 4205–4215.

(14) Brémondand, P.; Marque, S. R. A. First proton triggered C–ON bond homolysis in alkoxyamines. *Chem. Commun.* **2011**, *47*, 4291–4293.

(15) Bagryanskaya, E.; Brémond, P.; Edeleva, M.; Marque, S. R. A.; Parkhomenko, D.; Roubaud, V.; Siri, D. Chemically Triggered C–ON Bond Homolysis in Alkoxyamines. Part 2: DFT Investigation and Application of the pH Effect on NMP. *Macromol. Rapid Commun.* **2012**, *33*, 152–157.

(16) Brémond, P.; Koita, A.; Marque, S. R. A.; Pesce, V.; Roubaud, V.; Siri, D. Chemically Triggered C–ON Bond Homolysis of Alkoxyamines. Quaternization of the Alkyl Fragment. *Org. Lett.* **2012**, *14*, 358–361.

(17) Edeleva, M. V.; Kirilyuk, I. A.; Zhurko, I. F.; Parkhomenko, D. A.; Tsentalovich, Y. P.; Bagryanskaya, E. G. pH-Sensitive C–ON Bond Homolysis of Alkoxyamines of Imidazoline Series with Multiple Ionizable Groups As an Approach for Control of Nitroxide Mediated Polymerization. *J. Org. Chem.* **2011**, *76*, 5558–5573.

(18) Kirilyuk, I. A.; Bobko, A. A.; Grigor'ev, I. A.; Khramtsov, V. V. Synthesis of the Tetraethyl Substituted pH-Sensitive Nitroxides of Imidazole Series with Enhanced Stability towards Reduction. *Org. Biomol. Chem.* **2004**, *2*, 1025–1030.

(19) Zubenko, D.; Tsentalovich, Y.; Lebedeva, N.; Kirilyuk, I.; Roschchupkina, G.; Zhurko, I.; Reznikov, V.; Marque, S. R. A.; Bagryanskaya, E. Laser Flash Photolysis and CIDNP Studies of Steric Effects on Coupling Rate Constants of Imidazolidine Nitroxide with Carbon-Centered Radicals, Methyl Isobutyrate-2-yl and tert-Butyl Propionate-2-yl. *J. Org. Chem.* **2006**, *71*, 6044–6052.

- (20) Hodgson, J. L.; Roskop, L. B.; Gordon, M. S.; Lin, C. Y.; Coote, M. L. Side Reactions of Nitroxide-Mediated Polymerization: N–O versus O–C Cleavage of Alkoxyamines. *J. Phys. Chem. A* **2010**, *114*, 10458–10466.
- (21) Gryn'ova, G.; Marshall, D. L.; Blanksby, S. J.; Coote, M. L. Switching radical stability by pH-induced orbital conversion. *Nat. Chem.* **2013**, *5*, 474–481.
- (22) Gryn'ova, G.; Coote, M. L. Origin and Scope of Long-Range Stabilizing Interactions and Associated SOMO–HOMO Conversion in Distonic Radical Anions. *J. Am. Chem. Soc.* **2013**, *135*, 15392–15403.
- (23) Zhao, Y.; Truhlar, D. G. The M06 Suite of Density Functionals for Main Group Thermochemistry, Thermochemical Kinetics, Non-covalent Interactions, Excited States, and Transition Elements: Two New Functionals and Systematic Testing of Four M06-Class Functionals and 12 Other Functionals. *Theor. Chem. Acc.* **2008**, *120*, 215–241.
- (24) Tomasi, J.; Mennucci, B.; Cammi, R. Quantum Mechanical Continuum Solvation Models. *Chem. Rev.* **2005**, *105*, 2999–3094.
- (25) Ribeiro, R. F.; Marenich, A. V.; Cramer, C. J.; Truhlar, D. G. Use of Solution-Phase Vibrational Frequencies in Continuum Models for the Free Energy of Solvation. *J. Phys. Chem. B* **2011**, *115*, 14556–14562.
- (26) Improta, R.; Scalmani, G.; Barone, V. Quantum Mechanical Prediction of the Magnetic Titration Curve of a Nitroxide 'Spin Probe'. *Chem. Phys. Lett.* **2001**, *336*, 349–356.
- (27) Frisch, M. J.; Trucks, G. W.; Schlegel, H. B.; Scuseria, G. E.; Robb, M. A.; Cheeseman, J. R.; Scalmani, G.; Barone, V.; Mennucci, B.; Petersson, G. A. et al. *Gaussian 09*, revision A.1; Gaussian, Inc.: Wallingford, CT, 2009.
- (28) Coote, M. L.; Lin, C. Y.; Beckwith, A. L. J.; Zavitsas, A. A. A comparison of methods for measuring relative radical stabilities of carbon-centred radicals. *Phys. Chem. Chem. Phys.* **2010**, *12*, 9597–9610.
- (29) Poutsma, M. L. The Radical Stabilization Energy of a Substituted Carbon-Centered Free Radical Depends on Both the Functionality of the Substituent and the Ordinality of the Radical. *J. Org. Chem.* **2011**, *76*, 270–276.
- (30) Franzen, V. Beziehungen Zwischen Konstitution und Katalytischer Aktivität von Thiolaminen Bei der Katalyse der Intramolekularen Cannizzaro-Reaktion. *Chem. Ber.* **1957**, *90*, 623–633.
- (31) Fischer, H.; Kramer, A.; Marque, S. R. A.; Nesvadba, P. Steric and Polar Effects of the Cyclic Nitroxyl Fragment on the C–ON Bond Homolysis Rate Constant. *Macromolecules* **2005**, *38*, 9974–9984.
- (32) Iwao, K.; Sakakibara, K.; Hirota, M. J. Evaluation of Reactivity for Nitroxide Radical Trapping by Correlation Analysis Using Steric Substituent Parameter (Ω_s). *Comput. Chem.* **1998**, *19*, 215–221.
- (33) Beckwith, A. L. J.; Bowry, V. W.; Ingold, K. U. Kinetics of Nitroxide Radical Trapping. 1. Solvent Effects. *J. Am. Chem. Soc.* **1992**, *114*, 4983–4992.
- (34) Boury, V. W.; Ingold, K. U. Kinetics of Nitroxide Radical Trapping. 2. Structural Effects. *J. Am. Chem. Soc.* **1992**, *114*, 4992–4997.
- (35) Chateauneuf, J.; Luszyk, J.; Ingold, K. U. Absolute Rate Constants for the Reactions of Some Carbon-Centered Radicals with 2,2,6,6-tetramethyl-1-piperidinoxyl. *J. Org. Chem.* **1988**, *53*, 1629–1630.
- (36) Bagryanskaya, E. G.; Marque, S. R. A. Scavenging of Organic C-Centered Radicals by Nitroxides. *Chem. Rev.* **2014**, DOI: 10.1021/cr4000946.
- (37) Truhlar, D.; Garrett, B. Variational Transition State Theory. *Annu. Rev. Phys. Chem.* **1984**, *35*, 159–189.
- (38) Kiselev, V. G.; Gritsan, N. P. Theoretical Study of the Primary Processes in the Thermal Decomposition of Hydrazinium Nitroformate. *J. Phys. Chem. A* **2009**, *113*, 11067–11074.
- (39) Kiselev, V. G.; Cheblakov, P. B.; Gritsan, N. P. Tautomerism and Thermal Decomposition of Tetrazole: High-Level ab Initio Study. *J. Phys. Chem. A* **2011**, *115*, 1743–1753.
- (40) Henry, D. J.; Parkinson, C. J.; Mayer, P. M.; Radom, L. Bond Dissociation Energies and Radical Stabilization Energies Associated with Substituted Methyl Radicals. *J. Phys. Chem. A* **2001**, *105*, 6750–6756.
- (41) Hodgson, J. L.; Lin, C. Y.; Coote, M. L.; Marque, S. R. A.; Matyjaszewski, K. Linear Free-Energy Relationships for the Alkyl Radical Affinities of Nitroxides: A Theoretical Study. *Macromolecules* **2010**, *43*, 3728–3743.
- (42) Clark, K. B.; Wayner, D. D. M. Are Relative Bond Energies a Measure of Radical Stabilization Energies? *J. Am. Chem. Soc.* **1991**, *113*, 9363–9365.
- (43) Kirilyuk, I. A.; Bobko, A. A.; Khramtsov, V. V.; Grigor'ev, I. A. Nitroxides with Two pK Values - Useful Spin Probes for pH Monitoring within a Broad Range. *Org. Biomol. Chem.* **2005**, *3*, 1269–1274.
- (44) Reznikov, V. A.; Skuridin, N. G.; Khromovskikh, E. L.; Khramtsov, V. V. A New Series of Lipophilic pH-Sensitive Spin Probes. *Russ. Chem. Bull.* **2003**, *52*, 2052–2056; *Izv. Akad. Nauk. Ser. Khim.* **2003**, *52*, 1942–1946.